An Investigation of Polymer Diffusion in Hydrogel Laminates Using Near-Field FTIR Microscopy

Jennifer J. Sahlin[†] and Nikolaos A. Peppas*

School of Chemical Engineering, Purdue University, West Lafayette, Indiana 47907-1283

Received June 17, 1996; Revised Manuscript Received August 15, 1996[⊗]

ABSTRACT: The role of diffusion in gel/gel adhesion was examined by near-field FTIR microscopy. Using a near-field FTIR microscopy technique, compositional maps were obtained with improved spatial resolution and enhanced signal to noise ratio. With this technique, the resolution was enhanced by about a factor of 5. Polymer chain diffusion across a gel/gel interface was a substantial mechanism of adhesion. Diffusion of poly(ethylene glycol) (PEG) free chains across poly(acrylic acid) (PAA) gels was investigated. The diffusivity of PEG was on the order of 10^{-8} to 10^{-9} cm^2/s for these swollen polymer gels. PEG diffusivity in PAA gels scaled to $M^{-0.41}$. This was similar to values reported for PEG diffusion in aqueous solution.

Introduction

The process of gel/gel adhesion is significant in a variety of applications including thin film technology and bioadhesion. While the role of diffusion in un-cross-linked polymer systems has been studied, little is known about polymer diffusion in polymer networks[1] such as the mechanism of polymer diffusion in such systems or its impact on adhesion between two compatible polymers.

The role of diffusion in adhesion has been the topic of some discussion. Most of the data supporting this mechanism also agree with what would be anticipated by a wetting process. Thus, the effect of diffusion on hydrogel adhesion needs to be elucidated. Furthermore, the loosely cross-linked network of hydrogels may not exhibit behavior typical of either polymer melts or solutions. Thus, the dependence of the diffusivity on system parameters such as molecular weight, degree of cross-linking, and the degree of swelling are important if diffusion can be manipulated to enhance adhesion.

In the last 20 years, several IR spectroscopic techniques have been used to probe polymer−polymer diffusion. In their seminal work, Klein and Briscoe[2−4] used microdensitometry to investigate the diffusion of large molecules in polymers. Essentially, their experiment consisted of bringing two distinct polymers into contact, heating the system to various temperatures for specific time increments, and then quenching the sample to ambient temperature. Thin cross-sections were excised from the sample, and the concentration of the diffusant was monitored at an IR frequency which was unaffected by the bulk polymer. This was done by mounting a 90 ± 10 μm slit at the focus of the sample beam and setting the dispersive spectrometer at the desired frequency. An additive-free polymer sample was placed in the reference beam as an internal standard. The thin polymer section was slowly moved across the slit on a motorized stage, and the transmitted energy was recorded as a function of position. The estimated error in this technique was ±15%.

Klein and Briscoe[2−5] studied the diffusion of 0.5% stearamide in polyethylene at various times and temperatures and observed a discontinuity in the Arrhenius plot for temperatures above the melting point of PE. They also studied the translational diffusion of deuterated polyethylene in a protonated melt. Five distinct fractions of polyethylene were used. Diffusion was Fickian and independent of diffusant concentration up to 2 wt %. Furthermore, the average diffusion coefficient was inversely proportional to the square of molecular weight in agreement with DeGennes' reptation theory.

Since the development of FTIR spectroscopy, a variety of techniques has been used to monitor polymer−polymer diffusion, including transmission spectroscopy,[6] external reflection spectroscopy,[7] ATR spectroscopy,[8] and FTIR microscopy.[9] High *et al.*[6] presented a detailed analysis of the evaluation of the diffusion coefficient from an FTIR transmission experiment. Poly(ethylene-*co*-methacrylic acid) and poly(vinyl methyl ether) films which had been separately cast onto KBr windows were placed in intimate contact in a demountable transmission cell. The temperature was subsequently raised above the T_g of the polymer pair, and the spectra were recorded at various time increments. By following the fraction of carbonyl functional groups which are hydrogen bonded to the ether, the diffusion coefficient could be estimated. The technique of external reflection FTIR spectroscopy was used to study the interdiffusion of poly(vinyl chloride) (PVC) and poly(methyl methacrylate) (PMMA).[7] The interaction spectrum of the carbonyl stretch was followed as a function of time at elevated temperatures. This work clearly illustrated that changes occurred at the sampling depth of the technique, but the results were not analyzed quantitatively.

ATR-FTIR spectroscopy was used in conjunction with tensile strength measurements to verify that polymer interdiffusion enhanced adhesion in a PVC/PMMA system.[8] In these experiments, a PVC film was cast from a 1−2 wt % THF solution onto a glass plate. PMMA was then spin cast onto this layer to form a 1.5 μm film. This laminate was dried, floated onto water, and subsequently lifted onto a germanium ATR plate. The contact between the laminate and the crystal was improved during an annealing process which was done for various time intervals at 150 °C.

Klotz *et al.*[9] investigated the interdiffusion of poly(vinyl methyl ether) with $\bar{M}_n = 3200$, in polystyrene with $M_n = 800$, by following the interaction spectra as a function of time. This system was examined by following the changes in the ether stretch region in a polymer sandwich. The intensity of this band was fit to Fick's law and the diffusion coefficient was estimated.

* To whom correspondence should be addressed.

[†] Present address: Process Technologies Laboratory, 3M Corporate Research Labs, 3M Center, Building 208-1-01, St. Paul, MN 55101.

[⊗] Abstract published in *Advance ACS Abstracts,* October 1, 1996.

S0024-9297(96)00870-4 CCC: $12.00

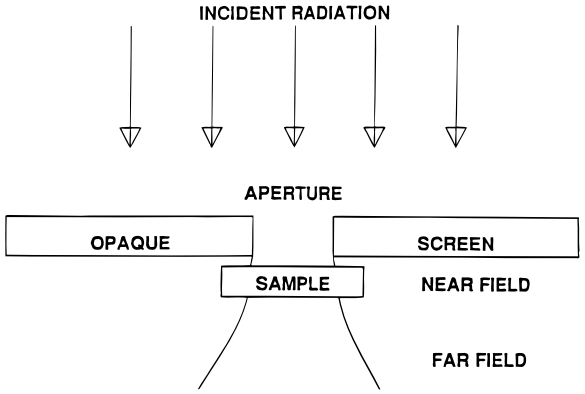

Figure 1. Schematic of the three optically distinct regions (incident radiation near field, far field) present when radiation impinges on an aperture.

More recently, Lustig and associates[10−12] have used ATR-FTIR spectroscopy to study diffusion in semicrystalline polymers and measure the polymer diffusion coefficients whereas Jabbari and Peppas[13,14] have analyzed ATR-FTIR spectroscopy data to determine concentration-dependent diffusion coefficients and non-Fickian transport in polymer/polymer systems.

The spatial resolution which can be achieved by using dual-aperturing FTIR microscopy is about 15 μm.[15,16] Generally, a high number of scans is required since the signal to noise ratio is low. Since polymer−polymer diffusion in highly compatible, un-cross-linked polymer pairs generally occurs on the micron scale, long contact times are required to use this technique. The spatial resolution and the signal to noise ratio can be improved by implementing near-field techniques.

The present research implements the technique of near-field FTIR spectral imaging to examine bulk diffusion of poly(ethylene glycol) (PEG) in poly(acrylic acid) (PAA) gels. The development of this technique is discussed elsewhere.[17] The essential feature of this technique is that the aperture which delineates the sampling region is moved to within a wavelength of the sample's surface.

Figure 1 shows three optically distinct regions surrounding an illuminated aperture. Each of these regions has unique dielectric properties, and each must be examined separately to determine the overall resolution limit of the system. A detailed analysis of this system was done by Betzig et al.[18] Essentially, light impinges upon an aperture. The light then passes through the slit or pinhole and becomes collimated due to the thickness of the aperture. When this light exits the aperture, it diffracts and spread out, forming an illumination cone. Generally, samples are studied in the far-field region of a microscope. In this regime, the resolution is limited by the wavelength of the light, since the radiation field from the sample contains structural information for wavelengths larger than $\lambda/2$. In the near-field region, on the other hand, the evanescent wave dictates the resolution since it contains structural information independent of the wavelength. The strength of the evanescent wave is, however, an exponential function of the distance from the sample. Thus, the resolution limit in the near-field is dictated by two factors: the separation distance and the detector sensitivity. Both of these parameters affect the minimum aperture size.

Experimental Part

Inhibited acrylic acid (AA) monomer (Aldrich, Milwaukee, WI) was vacuum distilled prior to the polymerization reaction.

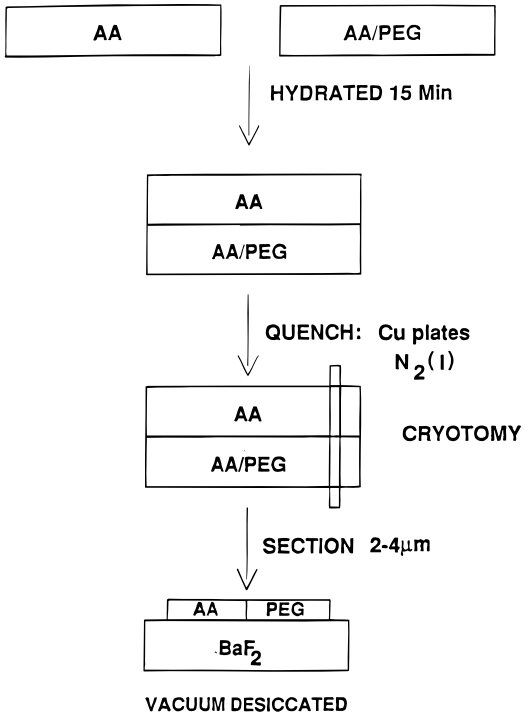

Figure 2. Schematic of the procedure used to prepare hydrogel laminates.

Since AA is highly reactive, the distillation was controlled by adding approximately 1 g of *N,N′*-diphenyl-1,4-phenylenediamine to 100 mL of AA. The additional inhibitor was essential to prevent the bottoms from polymerizing during the distillation process. The vacuum distillation was maintained at 34 °C and 5 mmHg. The photoinitiator 2,2-dimethoxy-2-phenylacetophenone (DMPA, Aldrich, Milwaukee, WI) and the cross-linking agent ethylene glycol dimethacrylate (EGDMA, Aldrich, Milwaukee, WI) were used as received.

A series of hydrogels was prepared for FTIR near-field microscopy experiments. UV, free radical, solution polymerization was used to incorporate aliquots of monodisperse PEG in PAA hydrogels. A monomer mixture containing 10 mol % AA and 90 mol % deionized water was prepared. The cross-linking agent to total monomer was constant at 0.005 mol of EGDMA/mol of EGDMA and AA. DMPA was added at 1 wt % of the monomer mixture. Finally, monodisperse PEG ($\bar{M}_n$ = 15 000, Polysciences, Warrington, PA, and Tosah, Tokyo, Japan) was added to the monomer mixture. The loading of PEG varied with the molecular weight of the PEG and was optimized for a strong infrared signal.

Disposable reaction molds were made by cutting gaskets out of rubber sheeting and gluing the gaskets onto microscope slides. The monomer mixture was then thoroughly agitated and poured into the molds, a second microscope slide was placed on top, and the sample was exposed to a UV source at approximately 5.5 mW/cm^2 for 3 min. The hydrogel formed was approximately 3 mm thick. Films were prepared containing aliquots of monodisperse PEG with molecular weights of $\bar{M}_n$ = 4250, 15 000, 26 000, 46 000, 85 000, 95 000, 570 000, and 885 000. The polydispersity indices, $\bar{M}_w/\bar{M}_n$, for these polymers were 1.03, 1.20, 1.20, 1.10, 1.06, 1.04, 1.10, and 1.08, respectively. PEG-free (unloaded) hydrogel films were also synthesized. These gels were used as the second layer in a laminate with a loaded film.

Hydrogel films prepared by UV polymerization were used for the spectral mapping experiments. Small sections of the PEG-loaded and neat PAA gels were swollen in deionized water for 5 or 15 min. The sections were subsequently trimmed to 5 mm × 10 mm and were stacked on top of each other. This laminate was placed between copper blocks and set inside a Pyrex dish (see Figure 2). The mass of the upper block was 31.75 g; thus, the pressure applied to the specimen was 6.2 kPa. The sample was maintained under this load for

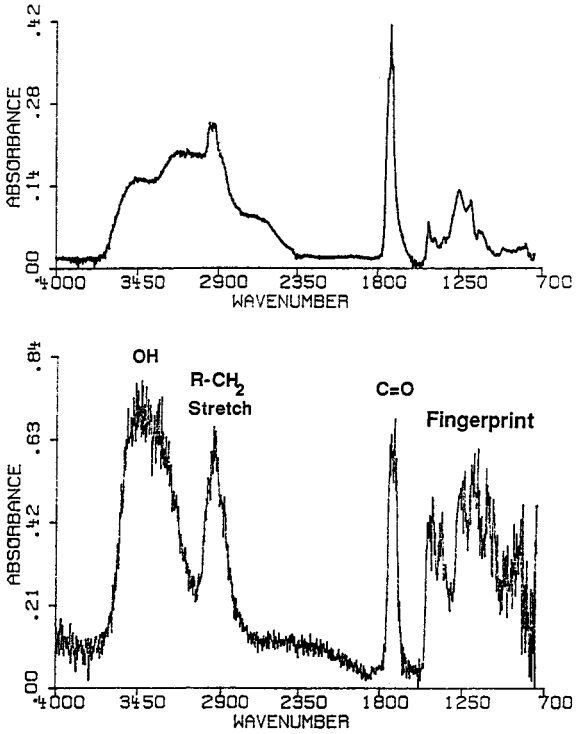

Figure 3. (a) FTIR spectrum of a near-field apertured 2 μm thick PAA section containing 0.005 mol of EGDMA/mol of AA and EGDMA mounted on a BaF_2 crystal. Conditions: aperture, 5 μm × 80 μm; 512 scans at 8 cm^{-1} resolution. (b) FTIR spectrum of a remotely apertured 4 μm thick PAA section containing 0.005 mol of EGDMA/mol of AA and EGDMA mounted on a BaF crystal. Conditions: aperture, 5 μm × 180 μm; 4096 scans at 8 cm^{-1} resolution.

a specified time period, henceforth designated as the contact time, *t*. Liquid nitrogen was then poured onto the copper blocks to quench the specimen and produced a rigid laminate of the two polymers which could then be mounted on a sample stub and sectioned using a cryotome. The polymer laminate was mounted on edge by fixing it to a metal stub with Tissue-Tek II (Lab-Tek Products, Naperville, IL) fluid.

The cryotome and the steel knife were maintained at −30 °C and 2 μm polymer sections were excised from the mounted laminate; the sample was cut with the interface moving toward the knife's edge to minimize sample deformation. The thin sections were then lifted off the knife with a BaF_2 crystal.

The concentration profile of the PEG in the PAA laminate was obtained by collecting a series of IR spectra using near-field FTIR spectroscopy, as described in detail elsewhere.[17] A BaF_2 crystal which supported the thin laminate sections was mounted on the motorized stage of an IR microscope. Small pieces of double-sided tape were used to secure the crystal; this prevented it from wiggling during the near-field experiment. For these experiments, the data were collected in 80 5 μm increments symmetrically positioned around the interface. When the system was properly aligned and tuned, the stage controller was used to collect spectra of the background and of the sample. These mapping experiments required approximately 6 h of collection time, primarily due to the number of scans collected for each position. Smooth peak shapes for integration were obtained by collecting 512 scans per spectrum.

Results and Discussion

When a polymer laminate was visually examined with a 10X or 15X microscope lens, a distinct interface between the two sections was observed. Although a visually diffuse boundary region did not form, interdiffusion of polymer segments could still occur, and this process would occur over a nanometer to micrometer length scale.

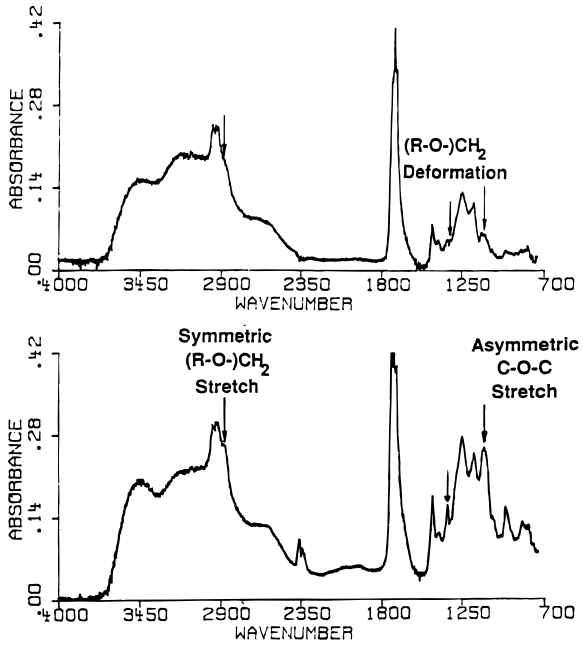

Figure 4. FTIR spectrum of a near-field apertured 2 μm thick section of unloaded PAA containing 0.005 mol of EGDMA/mol of AA and EGDMA (top) and a PEG ($\bar{M}_n$ = 15 000) loaded PAA network containing 0.005 mol of EGDMA/mol of AA and EGDMA (bottom). Conditions: aperture, 5 μm × 80 μm; 512 scans at 8 cm^{-1} resolution.

Figure 3a shows a spectrum of a 4 μm thick section of PAA on a BaF_2 crystal. The aperture dimensions were 5 μm × 80 μm, the spectrum was collected at 8 cm^{-1} resolution, and the sample was scanned 512 times. When this spectrum is compared with that shown in Figure 3b, it is clear that this technique offers a substantial enhancement. The reduction in stray light drastically improves the signal to noise. This reduces the number of scans required and also improves the clarity of the spectral details. The effect is most noticeable in the longer wavelengths (smaller wavenumbers) where diffraction effects have the most impact.

Figure 4 is a near-field FTIR spectrum of a PEG-loaded PAA network. The ether stretch from 1130 to 1040 cm^{-1} was used to map the concentration profile of PEG across the interface between the loaded and unloaded sections. The normalized −C−O−C− concentration as a function of position was fit in each case to Fick's second law with a constant diffusion coefficient and the following boundary conditions:

$$\frac{\partial C}{\partial t} = D\frac{\partial^2 C}{\partial^2 x} \tag{1}$$

where

$$t = 0 \qquad x < 0 \qquad C = C_0 \tag{2}$$

$$t = 0 \qquad x > 0 \qquad C = 0 \tag{3}$$

$$t = 0 \qquad x = 0 \qquad \frac{\partial C}{\partial x} = 0 \tag{4}$$

The solution of this form of Fick's law is

$$\frac{C(x,t)}{C_0} = {}^1/_2 \operatorname{erfc}\left[\frac{(x+h)}{2\sqrt{(Dt)}}\right] \tag{5}$$

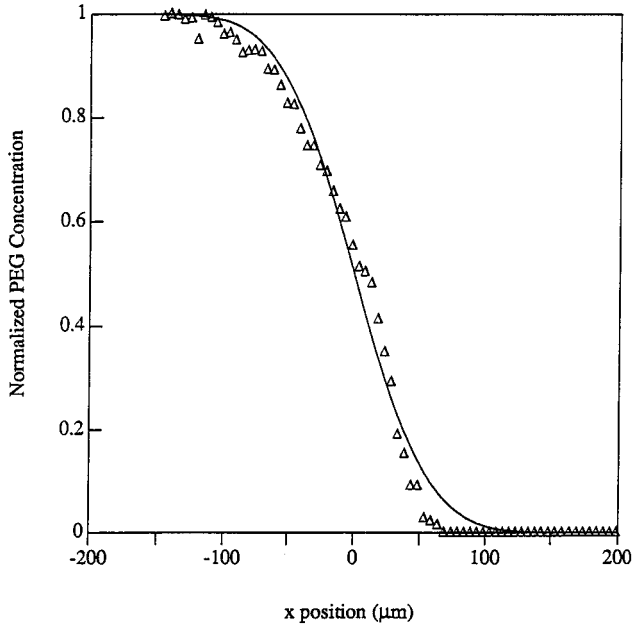

Figure 5. Normalized PEG concentration as a function of position. The PEG concentration was determined from the peak area of the asymmetric C−O−C stretch, 1130−1040 cm. Conditions: $\bar{M}_n$ = 15 000; contact time, 15 min; aperture, 5 μm × 80 μm; 512 scans at 8 cm^{-1} resolution. Solid line: solution of eq 5, $D = 1.1 \times 10^{-8}$ cm^2/s.

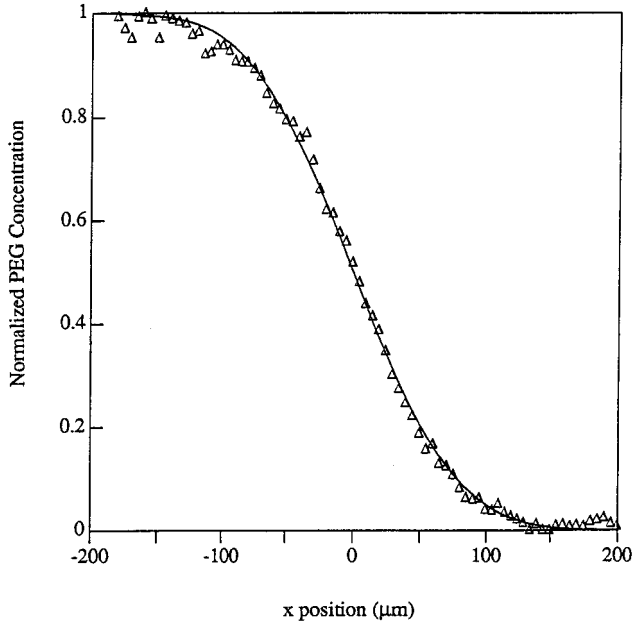

Figure 6. Normalized PEG concentration as a function of position. The PEG concentration was determined from the peak area of the asymmetric −C−O−C− stretch, 1130−1040 cm^{-1}. Conditions: $\bar{M}_n$ = 15 000; contact time, 30 min; aperture, 5 μm × 80 μm; 512 scans at 8 cm^{-1} resolution. Solid line: solution of eq 5, $D = 1.1 \times 10^{-8}$ cm^2/s.

where h is a shift factor which is required to ensure that at $x = 0$ and $C/C_0 = 0.5$.

The experimental results of PEG diffusion and the best fit of eq 5 are illustrated in Figures 5 through 7 for chain penetration (contact times) of 15, 30, and 90 min. The data were normalized so that the ordinate axes would be identical for all of these figures to clearly indicate that the interpenetration depth increased with contact time. The PEG diffusion coefficient, D, was calculated from these data.

Figure 8 is a log−log plot of the tracer diffusion coefficient for PEG diffusing through PAA networks as a function of PEG molecular weight. The regression results in which the sum-squared error was less than 0.2 are shown. The asymptotic 95% confidence intervals from the nonlinear regression are indicated on the figure as error bars. These results indicate that the near-field technique is an effective method for determining the tracer diffusion coefficient in polymer systems.

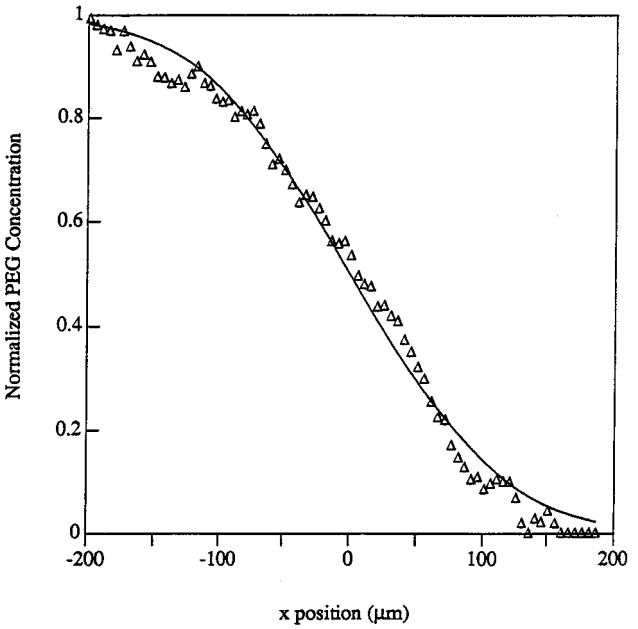

Figure 7. Normalized PEG concentration as a function of position. The PEG concentration was determined from the peak area of the asymmetric C−O−C stretch, 1130−1040 cm^{-1}. Conditions: $\bar{M}_n$ = 15 000; contact time, 90 min; aperture, 5 μm × 80 μm; 512 scans at 8 cm^{-1} resolution. Solid line: solution of eq 5, $D = 1.1 \times 10^{-9}$ cm^2/s.

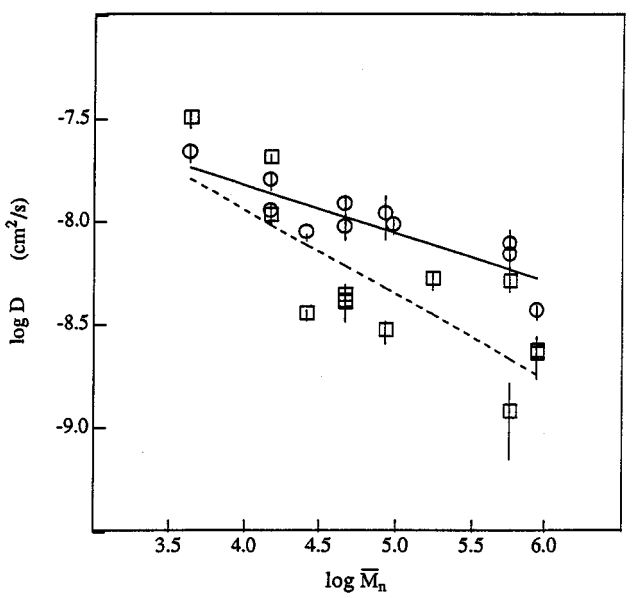

Figure 8. Tracer diffusion coefficient, D, as a function of PEG molecular weight, $\bar{M}_n$: (○) 15 min contact time; (□) 30 min contact time; (solid) $\alpha = -0.26$; (dashed) $\alpha = -0.41$.

The data of Figure 8 were fitted to

$$D = \beta M^{\alpha} \tag{6}$$

For a contact time of 15 min, the value of α was $\alpha = -0.23$ whereas at 30 min, it was $\alpha = -0.42$. There is substantial scatter in the data with respect to this regression analysis. This scatter is due to the variations

between samples which occurred during laminate preparation and sample contact.

The results are in reasonable agreement with the scaling behavior determined from dynamic light scattering experiments. For example, working with PEG of $\bar{M}_n$ 73 000 (significantly larger than ours), Brown[19] reported that the fast mode self-diffusion coefficient for PEG in aqueous solutions scaled to $\bar{M}_n^{-0.58}$. Furthermore, he found that the diffusion coefficient in aqueous solutions was 3.3×10^{-7} cm^2/s. This is approximately 1 order of magnitude higher than the values measured for PEG (with $\bar{M}_n = 15\,000$) in the loosely cross-linked PAA hydrogels examined in this research. The diffusivity of PEG in the PAA hydrogels is reasonable since the molecular chains of the gel would inhibit diffusion. Indeed, a calculation of the solvated end-to-end distance of PEG with $\bar{M}_n = 15\,000$ and a $C_n = 14.6$, as reported before,[20] indicated a value of $r = 49.8$ Å. Similarly, the mesh size of the PAA networks used here was $r' = 228.8$ Å. The resulting restriction coefficient $\lambda = 0.43$ indicates an expected PEG diffusion coefficient reduction of 1 order of magniude. Any complexation between the PEG and PAA would repress the diffusion process even though the pH of the swelling medium was above the polymer's pK_a.

Rotstein and Lodge[1] observed markedly different scaling behavior with $D \sim M^{-2.8}$ for polystyrene diffusing through cross-linked poly(vinyl methyl ether) gels. Their data analysis clearly indicated that the scatter in the data is a function of the degree of cross-linking. In fact, Rotstein and Lodge scaled their tracer diffusion coefficients by a factor of $\langle M_c \rangle / M_c$ where $\langle M_c \rangle$ is the expected molecular weight between cross-links and M_c is the actual value for the gel examined. This method of scaling the diffusivities was not feasible for the PAA system since the actual M_c could not be determined from swelling studies for this system.

The cross-linking ratio used by Rotstein and Lodge[1] was varied from 25:1 to 50:1 to 100:1. In our PEG/PAA study, however, a constant cross-linking ratio of 200:1 was used. Since the average number of monomer units for entanglement is $N_e \sim 200$, the molecular weight between entanglements for PAA is approximately 14 400. However, the value of the molecular weight between cross-linked M_c for the cross-linking ratio used in these experiments is 7200. Thus, $M_c < M_e$, and the topological constraints of the network are dictated by the cross-links in the network. It is important to note, however, that the anionic nature of the gel used in these studies may affect the diffusion process since these gels exhibit substantially enhanced swelling when the pH > pK_a (PAA).

The ether/acid interaction which may occur in the PEG/PAA system was investigated by examining the carbonyl region of several locations extracted from an interfacial mapping experiment for a laminate sample. Figure 9 shows the region from 1540 to 1900 cm^{-1} for a laminate prepared from neat PAA and PEG-loaded ($\bar{M}_n$ =15 000) PAA. The contact time for this sample was 30 min. The top spectrum is from the bulk PAA region while the bottom spectrum is from the PEG-loaded region. The $\bar{\nu}$(COOH) absorption in the bulk PAA is at approximately 1700 cm^{-1}; this band is due to self-association between the acid groups in the polymer matrix. In the loaded region, two apparently separate carbonyl stretching modes are discernible: one at approximately 1714 cm^{-1} and the second near 1735 cm^{-1}. The band at 1735 cm^{-1} is due to hydrogen bonding between the ether oxygen and the hydrogen atom of the carboxylic acid. High *et al.*[6] successfully monitored the change in peak area for these two distinct bands at 2 cm^{-1} resolution. The three intermediate peaks shown in Figure 9 are not readily interpretable since these spectra were collected at 8 cm^{-1} resolution. The spectral results at 2 cm^{-1} resolution, however, indicated that only one peak was present. Thus, the fine structure which is clearly evident in Figure 9 is due to the limited resolution of the spectra.

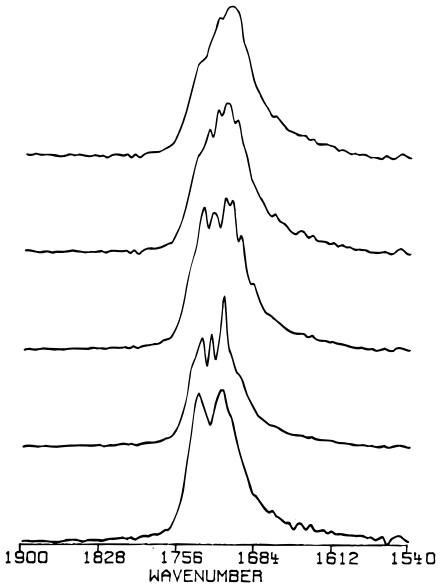

Figure 9. Carbonyl region of the near-field FTIR spectra collected at 8 cm^{-1} resolution for various positions relative to the laminate interface. The probe molecular weight was 15 000, and the contact time was 15 min. The top spectrum is of the PAA region, and the bottom spectrum is the PEG-loaded PAA region. The intermediate spectra are for regions in the interdiffusion zone.

The mapping experiments with this polymer pair indicate a dimerization of PAA which may also be somewhat affected by association with PEG or by a swelling medium with a pH higher than the polymer's pK_a. The ionization of the PAA network was examined in a pH 10 medium to see if the observed dimerization persists in a more basic environment. A strong peak centered at ~1640 cm^{-1} and a peak between 1700 and 1745 cm^{-1} were readily apparent in the carbonyl region of the difference spectrum of the gel; the 1580 and 1640 cm^{-1} peaks are due to the COO^- ion. The shift of the primary carbonyl band to lower frequencies indicates that the dimerization of PAA can be substantially reduced in highly basic medium.

The dependence of the PEG diffusion coefficient on contact time at a constant tracer molecular weight of 15 000 is illustrated in Figure 10. This log−log plot shows that the diffusion coefficient decreases with contact time. The diffusion coefficient at this PEG molecular weight is inversely proportional to time. This is an unexpected result and may be due to sample drying during the contact time. The mobility would be lower in a less swollen network. As a result, the diffusion of PEG would be slowed by the drying process, and this would lead to a lower diffusivity at longer contact times. With these data we do not mean to imply a diffusional time dependence but probably a relaxational (chain rearrangement) process. Finally, it must be noted that the PAA samples were loaded with 15 wt % PEG. This is substantially higher than the 2 wt %

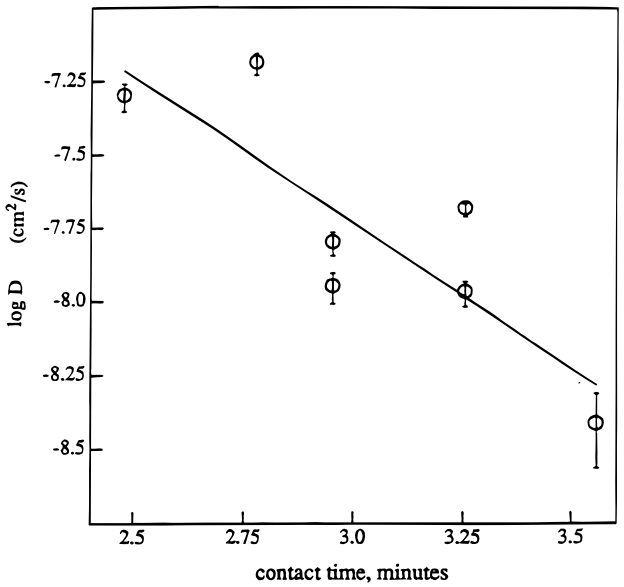

Figure 10. Diffusivity, D, as a function of time at constant molecular weight, $\bar{M}_n$ = 15 000: (○) measured diffusivity; (solid) $D-t^{-1}$.

loading used by Klein and Briscoe.[3,4] However, the intensity of the infrared signal is a function of the number of IR active groups. As a result, the signal is a function of the molar loading.

Conclusions

Diffusion can be effectively monitored in polymer systems by using near-field FTIR microscopy. In this investigation, the diffusion of a probe molecule across a gel/gel interface was studied. Diffusion occurs over the micrometer range in hydrogel laminates.

The diffusion process observed in this research is distinctly different from what has been previously reported for polymer gels which do not hydrogen bond. The results do correlate fairly well with dynamic light scattering measurements of PEG self-diffusion in aqueous solution. The diffusivity scaled as $M^{-0.42}$ for a constant contact time of 30 min. The diffusion coefficient is approximately 1 order of magnitude lower for diffusion in the hydrogel systems.

The diffusion coefficient also scaled as t^{-1} for $\bar{M}_n$ =15 000. The PAA was protonated during these mapping experiments. As a result, hydrogen bonding between the PEG and the PAA could occur during the diffusion process. This was not observed, however, when the polymer sections were examined with 2 cm^{-1} resolution.

Acknowledgment. This work was supported by grant No. GM 45027 from the National Institutes of Health.

References and Notes

(1) Rotstein, N. A.; Lodge, T. P. *Macromolecules* **1992**, *25*, 1316−1325.
(2) Klein, J.; Briscoe, B. J. *Nature* **1975**, *257*, 386−387.
(3) Klein, J.; Briscoe, B. J. *Polymer* **1976**, *17*, 481−484.
(4) Klein, J. *Nature* **1978**, *271*, 143−145.
(5) Klein, J.; Briscoe, B. J. *Proc. R. Soc. London, Ser. A.* **1979**, *356*, 53−73.
(6) High, M. S.; Painter, P. C.; Coleman, M. M. *Macromolecules* **1992**, *25*, 797−801.
(7) Boven, G.; Brinkhuis, R. H. G.; Vorenkamp, E. J.; Schouten, A. J. *Macromolecules* **1991**, *24*, 967−969.
(8) Vorenkamp, E. J.; van Ruiten, J.; Kroesen, F. A.; Meyer, J. G.; Hoekstra, J.; Challa, G. *Polym. Commun.* **1989**, *30*, 116−120.
(9) Klotz, S.; Cantow, H.-J.; Knopf, M. In *Intergration of Fundamental Polymer Science and Technology*; Lemstra, P. J.; Kleintjens, L. A., Eds.; Elsevier: Amsterdam, 1986; pp 252−256.
(10) Van Alsten, J. G.; Lustig, S. R. *Macromolecules* **1992**, *25*, 5069.
(11) Lustig, S. R.; Van Alsten, J. G.; Hsiao, B. *Macromolecules* **1993**, *26*, 3885.
(12) Van Alsten, J. G.; Lustig, S. R.; Hsiao, B. *Macromolecules* **1995**, *28*, 3672.
(13) Jabbari, E.; Peppas, N. A. *Macromolecules* **1993**, *26*, 2175.
(14) Jabbari, E.; Peppas, N. A. *J. Adhesion* **1993**, *43*, 101.
(15) Messerschmidt, R. G. In *The Design, Sample Handling, and Applications of Infrared Microscopes*; Roush, P. B., Ed.; ASTM STP, 949; American Society for Testing and Materials: Philadelphia, PA, 1987; pp 12−26.
(16) Messerschmidt, R. G. In *Infrared Microspectroscopy: Theory and Applications*; Messerschmidt, R. G., Harthcock, M. A., Eds.; Marcel Dekker: New York, 1988; pp 1−19.
(17) Sahlin, J. J.; Peppas, N. A. *J. Appl. Polym. Sci.*, in press.
(18) Betzig, E.; Harootunian, A.; Lewis, A.; Isaacson, M. *Appl. Opt.* **1986**, *25*, 1890−1900.
(19) Brown, W. *Macromolecules* **1984**, *17*, 66−72.
(20) Bell, C. L.; Peppas, N. A. *Biomaterials* **1996**, *17*, 1203−1218.

MA960870U